# Efficient Loop Closure based on FALKO LIDAR Features for Online Robot Localization and Mapping

Fabjan Kallasi[1] and Dario Lodi Rizzini[1]

***Abstract*— Keypoint features detection from measurements enables efficient localization and map estimation through the compact representation and recognition of locations. The keypoint detector FALKO has been proposed to detect stable points in laser scans for localization and mapping tasks. In this paper, we present novel loop closure methods based on FALKO keypoints and compare their performance in online localization and mapping problems. The pose graph formulation is adopted, where each pose is associated to a local map of keypoints extracted from the corresponding laser scan. Loops in the graph are detected by matching local maps in two steps. First, the candidate matching scans are selected by comparing the scan signatures obtained from the keypoints of each scan. Second, the transformation between two scans is obtained by pairing and aligning the respective keypoint sets. Experiments with standard benchmark datasets assess the performance of FALKO and of the proposed loop closure algorithms in both offline and online localization and map estimation.**

## I. INTRODUCTION

The recognition of distinctive regions and places from sensor measurements is a fundamental capability in robot localization and mapping problems. When the robot comes back to an already visited region after travelling a long path, this operation is commonly named loop closure and is crucial to globally localize the robot and to achieve consistent maps. Beyond place recognition, an additional requirement of loop closure is the computation of the relative transformation between the current robot frame and the matching one. Although this topic has been extensively investigated, place recognition with range finder is comparatively less developed than in the case of computer vision or other sensor data. Planar laser scans provide limited information beyond metric and occupancy data and, therefore, loop closure has been mainly addressed by matching occupancy grid maps [1]–[4].

Recently, two keypoint features specific for planar range finders have been proposed, namely FLIRT [5] and FALKO [6], allowing lightweight maps. If scans are represented as collections of points, then the problem of detecting loops in robot trajectory is reformulated as a comparison between a query point set and all the stored point sets of the map. Since point-to-point association is a computationally complex procedure, the exhaustive matching of point sets has been substituted by the efficient comparison of scan signatures. A signature is a vector obtained from the keypoints detected from a laser scan that can be used to select candidate loops. The state-of-the-art signatures are geometrical FLIRT phrase (GFP) [7], inspired by bag-of-word techniques, geometric landmark relations (GLARE) [8], and geometrical surface relations (GSR) [9]. These works also implicitly sketch a loop closure procedure in two steps: the selection of candidate loops using signatures and the point-to-point association to estimate the transformation. However, since each work is focused on a specific aspect, the experiments presented there do not properly highlight the contribution of the keypoint detector, the signature-based selection, and the point-to-point association to the solution of loop closure. It would be convenient to measure how keypoint stability, geometric patterns and point correspondences affect place recognition. Moreover, the experimental assessments of these methods [6]–[9] is usually conceived to highlight scan retrieval capabilities rather than to solve real online localization and mapping. During the online exploration, the scan dataset available for loop closure includes only the already acquired scans (causality). Effective reduction of localization uncertainty is achieved only by large loops rather than by matching consecutive or sequentially close scans (time discontinuity).

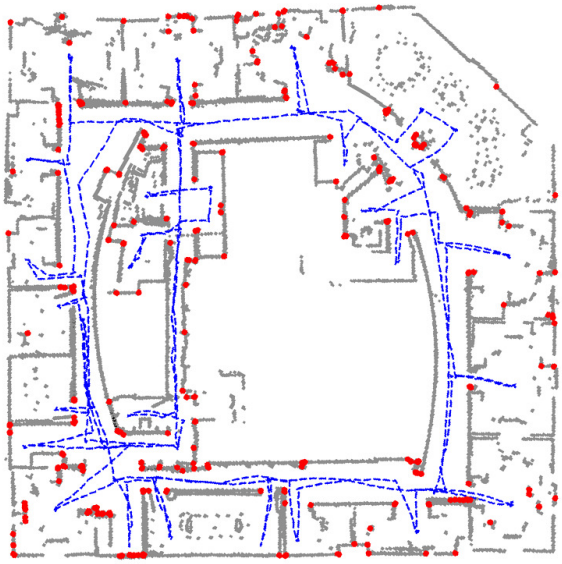

Fig. 1: Example of FALKO keypoint (red points) extraction in *intel-lab* dataset.

In this paper, we present novel loop closure methods based on FALKO keypoints (Fig. 1) and compare their performance in online localization and mapping problems. The methods based on geometric constraints like GLARE

[1]Authors are with RIMLab - Robotics and Intelligent Machines Laboratory, Dipartimento di Ingegneria dell'Informazione, University of Parma, Italy, {kallasi,dlr}@ce.unipr.it

signatures and point-to-point correspondences better perform with stable and viewpoint-invariant keypoints like FALKO. The loop closure procedures considered in our experimental assessment are obtained by combining a keypoint detector, a signature and a point-to-point association algorithm. The considered keypoints are FLIRT and an improved version of FALKO detector that computes point coordinates with subbeam accuracy. The scan signatures include the state-of-the-art GFP, GSR, and GLAROT, a novel version of GLARE fully invariant to rigid transformation. The tested point-to-point association algorithms are RANSAC, Correspondence Graph approach and Affine Hough Transform. Experiments illustrate the performance of discussed methods in the context of both onffline and online loop closure, i.e. both disregarding and considering causality and time discontinuity constraints in scan association. Moreover, the loop closure methods are applied to online map estimation.

## II. RELATED WORK

The approaches to data association and loop closure are strongly dependent on the map model. Occupancy grid maps are the most common representation for planar range finders due to the limited information provided by such sensor data. Thus, correlation-based techniques are the earlier data association methods used to match grid maps [1], [2]. To overcome the frequent loop closure errors resulting from gridmap matching, several expedients have been developed including lazy data association [3] and accurate sample management when using Rao-Blackwellized Particle Filters [4].

The recent proposal of keypoint features for planar range finders has enabled adaptation of pairing methods designed for features and landmarks. Bosse and Zlot proposed the first keypoint detector by processing a scan-based submap [10] and investigated the problem of matching features for loop closure [11]. The laser scan features presented in [12] are obtained by converting the laser scan into an image and by detecting Kanade-Tomasi corners. To overcome the inaccuracy due to rasterization, the method is improved in scan preprocessing, corner extraction and candidate suppression [13]. Tipaldi and Arras [5] proposed FLIRT, the first keypoint feature explicity designed for planar laser scans. FLIRT interest points are detected from the rescaled copies of the input laser scan and are provided with descriptors encoding the local distribution of neighbor points. While FLIRT is a practical and conceptual improvement over the previous approaches, keypoint detection is only based on the scan curvature, which may result into the identification of multiple and potentially unstable interest points. FALKO detector [6] extracts fast and stable keypoints from a laser scan through the selection of neighbors in the scan and the computation of a cornerness score. In these works, each keypoint is associated to a corresponding descriptor, a signature of the keypoint which is dependent on the keypoint neighborhood for more robust associations. However, the experiments presented in [5], [6] demonstrate the weakness of pure descriptor-association due to the intrinsic lack of information in laser scan data.

Range finder features enable data association according to the pairing-driven approach. Pairing algorithms produce explicit pairs of corresponding features and include joint compatibility test [14], Correspondence gGraph [15] and affine Hough-based assocation [16]. However, point-to-point association is fast, robust and feasible only between small point sets thus the keypoints are usually collected into smaller local maps. Several state-of-the-art methods address global localization and loop closure problems by matching signatures, which encode the relations between the keypoints of a local map. Tipaldi et al. [7] propose geometrical FLIRT phrases (GFPs) to represent the keypoints detected in a laser scan. GFPs extend the bag-of-words techniques, popular in computer vision, to planar range finders using FLIRT descriptors. Instead of relying on the weak descriptors, Geometric LAndmark RElations (GLARE) [8] are based on geometric invariants in a keypoint set like pairwise distances and angles. Although robust, GLARE signature is not invariant to rotation, and geometrical surface relations (GSR) have been proposed to overcome this limitation [9]. The loop closure performance of these signatures depends on the stability of the keypoints detected from the range scans.

## III. FALKO KEYPOINTS

In this section, we summarize FALKO, a keypoints extractor for laser scan which exploits the concept of edge intersection in 2D range data. In particular, this extractor has been designed to extract stable interest points like *corners* present in the environment and to be orientation invariant and point density independent. Finally, an improved variant of FALKO keypoints with subbeam accuracy is presented.

### A. FALKO Extractor

Let $\mathcal{S}$ be the point set from an input laser scan and $p_i \in \mathcal{S}$ ($i$ index in the scan) a candidate interest point of the scan. The neighborhood of each candidate scan point $p_i$ is defined as $C(p_i) = \{p_j \in \mathcal{S} : \|p_j - p_i\| \leq r_i\}$, where $r_i$ is a radius which increases with $\|p_i\|$, the distance from the sensor origin of the considered point. Thus, an approximately uniform number of neighbors for $p_i$ is guaranteed. In our implementation, the radius is computed as $r_i = a \exp(b\|p_i\|)$ where the parameters $a = 0.2$ and $b = 0.07$ are chosen s.t. $0.20\ m \lesssim r_i \lesssim 0.40\ m$ for ranges in $1 - 10\ m$.

A set of geometric considerations avoids evaluation of points which cannot be considered as candidate corners due to the lack of neighbors, geometric inconsistency or artifacts originated by range discontinuities. For each point $p_i$, the point set $C(p_i)$ is divided in two subsets

$$C_L(p_i) = \{p_j \in C(p_i) : j < i\} \quad (1)$$

$$C_R(p_i) = \{p_j \in C(p_i) : j > i\} \quad (2)$$

The first consideration is based on the cardinality of the two subsets. If $|C_L| < 2$ or $|C_R| < 2$, the point is discarded from the candidate corner set. For each remaining candidate

points, two neighborhood endpoints $x_L$ and $x_R$ are defined:

$$x_L = p_{j_{min}} : \quad j_{min} = \arg\min_j \{p_j \in C_L(p_i)\} \tag{3}$$

$$x_R = p_{j_{max}} : \quad j_{max} = \arg\max_j \{p_j \in C_R(p_i)\} \tag{4}$$

The triangle $\triangle p_i x_L x_R$ is then evaluated as a rough approximation of the corner. Let $\overline{x_L x_R}$ be the base of the triangle. If the base length $\|\overline{x_L x_R}\|$ or the triangle height is less than $\frac{r_i}{\beta}$ the point is discarded. Parameter $\beta$ is chosen taking into account specific limitations on the aperture and subtended angle of the corner. In particular, greater values of $\beta$ allow both wider and sharper corners to be selected as candidates. These conditions efficiently filter unsuitable corner candidates based on simple geometric properties. Then, for each candidate point which has passed the geometric verifications, a *cornerness* score is computed. A polar grid, which quantizes the space in circular sectors, is centered on the candidate point $p_i$. For each point $p_{j,L} \in C_L(p_i)$ and $p_{j,R} \in C_R(p_i)$, a quantized orientation w.r.t. the candidate point is computed as

$$\phi_{j,L} = \left\lfloor \frac{s_n}{2\pi} \ \tan^{-1}\left(\frac{p_{j,y} - p_{i,y}}{p_{j,x} - p_{i,x}}\right) \right\rfloor, \quad \forall p_j \in C_L(p_i) \tag{5}$$

$$\phi_{j,R} = \left\lfloor \frac{s_n}{2\pi} \ \tan^{-1}\left(\frac{p_{j,y} - p_{i,y}}{p_{j,x} - p_{i,x}}\right) \right\rfloor, \quad \forall p_j \in C_R(p_i) \tag{6}$$

where $s_n$ is the number of circular sectors in the polar grid. Let

$$d_\theta(\phi_1, \phi_2) = \left((\phi_1 - \phi_2) + \frac{s_n}{2}\right) (\text{mod } s_n) - \frac{s_n}{2} \tag{7}$$

be a distance function between the quantized orientations in circular sector units. The score for a candidate point is defined as

$$score_L(p_i) = \sum_{h=i-1}^{j_{min}} \sum_{k=h-1}^{j_{min}} |d_\theta(\phi_h, \phi_k)| \tag{8}$$

$$score_R(p_i) = \sum_{h=i+1}^{j_{max}} \sum_{k=h+1}^{j_{max}} |d_\theta(\phi_h, \phi_k)| \tag{9}$$

$$score(p_i) = score_L(p_i) + score_R(p_i) \tag{10}$$

The score function (10) measures the alignment of the two point sets $C_L$ and $C_R$ and it is orientation invariant. For each set, the more points are aligned in the same *direction* the smaller is the score value. Keypoints are then chosen as local minima of the score function in (10) with a non-maxima suppression procedure with range $0.20\ m$.

### B. Subbeam Accuracy

FALKO extractor select a sets of keypoints $kp_i \in \mathcal{S}$ from the laser scan $\mathcal{S}$. Unfortunately, those keypoints are not guaranteed to represent the exact edge generating the corner. Indeed, due to the discrete quantization of the laser scan, two consecutive laser beams can miss the corner edge and hit respectively the right and left sides of the edge. To increase the detection accuracy and the stability of the keypoint, a *subbeam* evaluation is performed. The subbeam accuracy is reached approximating the two subsets $\{C_L(kp_i); kp_i\}$ and $\{C_R(kp_i); kp_i\}$ with respectively two lines, $l_L$ and $l_R$. The approximation is performed with a least-square regression over the point subset. The intersection of the two lines gives the new keypoint $kp_i^\star$. To avoid mismatch of the subbeam detection due to outliers in the least-square regression, the new keypoint coordinates $kp_i^\star$ are accepted only if not too far from the former evaluation $kp_i$ ($\|kp_i^\star - kp_i\| < 0.2m$).

## IV. LOOP CLOSURE METHODS

The detection of stable features from laser scans can be exploited to build lightweight maps alternative to the traditional occupancy grid maps. While in principle each feature could be used as an independent landmark in a global map, point association becomes more robust when points extracted from a laser scan are collected into local maps. The point-to-point association among the keypoints of consecutive scans can rely on the relative pose estimation between the two frames given by odometry. However, when the robot comes to an already visited region after travelling a long path and closes a loop, the estimation of point correspondences becomes more difficult due to the larger uncertainty of robot pose. Thus, loop closure should exploit invariants like the mutual geometric relations of the keypoints in a local map.

In this work, a graph of local maps is used, where each local map is built from a laser scan and the local map frame is the robot frame from which the laser measurement has been acquired. Each local map consists of the stable FALKO keypoints extracted from the corresponding laser scan. To make loop closure efficient, a vector of real values called signature is computed for each keypoint map. We propose GLAROT signature, a variant of GLARE signature [8] that is provided with a novel rotation invariant metric. The loop closure procedure is performed in two steps: selection of candidate loops and keypoint-to-keypoint assocation. First, candidate loops are selected by comparing the signatures of current local map with the other signatures in the database according to the metric. Second, point-to-point association is performed to validate candidate loops and to compute the transformation between the current and candidate map frames. In the remaining of this section, we illustrate the GLAROT signature and two point-to-point association methods: Correspondence Graph (CG) and Affine Hough Transform (AH).

### A. GLAROT Signature

The Geometric landmark relations (GLARE) algorithm computes a signature that encodes the pairwise distances and angles of a point set. This method only requires the coordinates of the input points and no other information like descriptor values often provided by keypoint features. Given a set of 2D points $\mathcal{P}$, the pairwise angles and distances of two different points $p_i, p_j \in \mathcal{P}$ (assume that $p_{i,y} > p_{j,y}$) are defined respectively as

$$\theta_{ij}^+ = \text{atan2}(p_{i,y} - p_{j,y}, p_{i,x} - p_{j,x}) \qquad \rho_{ij} = \|p_i - p_j\| \tag{11}$$

GLARE signature encodes all the above pairwise relations into an accumulator array $G$ similar to the Hough transform

one [17]. $G$ consists of $n_\theta \times n_\rho$ cells with an assigned size $\Delta\theta \times \Delta\rho$ and the accumulator $S_g(t,r)$ is associated to each cell, where $t$ and $r$ are the indices of the cell. If the pairwise angle $\theta_{ij}^+$ and distance $\rho_{ij}$ belong to a cell $(t,r)$, then the corresponding $G_{t,r}$ is incremented. To take into account the point uncertainty, the accumulators of adjacent cells are also incremented by the values obtained by sampling a Gaussian function centered in $(\theta_{ij}^+, \rho_{ij})$.

The similarity between a source point set $\mathcal{P}^S$ and a target one $\mathcal{P}^T$ is measured by the distance between the respective signatures $G^S$ and $G^T$ according to $L_1$ norm [8]. Unfortunately, GLARE signature is invariant only to translation, but not to rotation. To overcome this problem, the GSR signature [9] estimates the normal direction of the implicit surface from which points are sampled by the laser scan. The normal angle is computed by collecting the points of the original scan into an Euclidean grid and by finding the normal distribution of the points lying inside a cell. The novel pairwise angles $\theta_{ij}^*$ are defined as the differences between normal angles. While rotational invariant, the computation of GSR is expensive due to the adoption of a grid and is less general than GLARE.

To make GLARE rotation invariant we propose GLAROT (GLAre ROTation-invariant), a novel procedure for comparing GLARE signatures. A rotation of the point set about an angle $\beta$, shifts the values of pairwise angles from $\theta_{ij}^+$ to $\langle\theta_{ij}^+ + \beta\rangle_\pi$, where $\langle x\rangle_m$ is the $m$ modulo operator. The angular shifts discretized with cell resolution $\Delta\theta$ are executed as circular shifts of an array. Even though the rotation angle $\beta$ between two point sets $\mathcal{P}^S$ and $\mathcal{P}^T$ is unknown, it can be recovered by searching for the angular shift that minimizes the distance between the signatures $G^{S,k}$ and $G^T$, where $G^{S,k}$ is obtained through a circular shift on the columns of $G^S$. In particular, the *shifted* $L_1$ *norm* ($SL_1$) is defined as

$$SL_1(G^S, G^T) = \min_k \sum_{t=0}^{n_\theta - 1} \sum_{r=0}^{n_\rho - 1} \left| G_{t,r}^T - G_{\langle t+k\rangle_{n_\theta}, r}^S \right| \qquad (12)$$

The computation of $SL_1$ requires $n_\theta$ evaluations of $L_1$ norm for $k = 0, \ldots, n_\theta - 1$. In practice, since the standard value of $n_\theta$ is 8, such operation is faster than the computation of normals needed by GSR.

### B. Correspondence Graph

The signature comparison makes an initial fast selection of candidate local maps for loop closure. However, the validation of such candidates and the estimation of the rigid transformation between local maps require point-to-point associations between point sets. The most effective methods for point correspondences do not depend on the initial estimation of relative pose between the local maps, but compare the internal mutual relations among the points of each set. The distance between point pairs is an example of geometric relation internal to a point set. Correspondences between the points of two sets are considered valid only if their internal relations are compatible.

The *Correspondence Graph* method [15] provides an elegant way to represent both the point set internal relations and the associations using graphs. Let $\mathcal{P}^S$ and $\mathcal{P}^T$ be respectively the source and target point sets. Let $\rho_{i_s,j_s}^S$ be the Euclidean distance between $p_{i_s}^S, p_{j_s}^S \in \mathcal{P}^S$ for $i_s \neq j_s$. All the pairs of $p_{i_s}^S$ and $p_{j_s}^S$ and their distances are collected into set $\mathcal{E}^S$. The feature graph of the source point sets is the complete undirected graph with vertices $\mathcal{P}^S$ and with edges $\mathcal{E}^S$. The feature graph of target point set with vertices $\mathcal{P}^T$ and edges $\mathcal{E}^T$ (within mutual distances $\rho_{i_t,j_t}^T$) is similarly defined.

The correspondence graph is defined as follows. A vertex $v_{i_s,i_t}$ of the correspondence graph represents the association between points $p_{i_s}^S \in \mathcal{P}^S$ and $p_{i_t}^T \in \mathcal{P}^T$. Two vertices $v_{i_s,i_t}$ and $v_{j_s,j_t}$ are connected by an edge *iff* the internal relations of $p_{i_s}^S$ with $p_{j_s}^S$ and of $p_{i_t}^T$ with $p_{j_t}^T$ are compatible. In particular, there is compatibility when their distances are equal up to a tolerance $\epsilon$, i.e. if $|\rho_{i_s,j_s}^S - \rho_{i_s,j_s}^T| < \epsilon$. The reliability of point-to-point data association increases with the number of mutually compatible associations. Thus, the optimal solution is given by the maximum set of mutually compatible associations, i.e. the maximum clique of the correspondence graph.

### C. Hough Data Association

Point-to-point association can be exploited using a voting method based on the Generalized Hough Transform [16], [18]. The proposed algorithm uses a generalization of the Hough transform for affine matrices representing 2D rigid transformations. In particular, each element in the Hough space is indexed with a parameter vector $\mathbf{v} = [t_x, t_y, \theta]^\top$ which characterizes the corresponding affine transform. For computational reason, the Hough space is bounded in $[\mathtt{min}_x, \mathtt{max}_x] \times [\mathtt{min}_y, \mathtt{max}_y] \times [\mathtt{min}_\theta, \mathtt{max}_\theta]$ and each parameter is quantized with respectively three steps $\Delta_x$, $\Delta_y$ and $\Delta_\theta$. Thus, the Hough space is represented by a three dimensional matrix where each element stores the matching pairs subset which is compatible with the corresponding quantized affine transform. As in section IV-B, let $\mathcal{P}^S$ and $\mathcal{P}^T$ be respectively the source and target point sets. Let $p_i^S \in \mathcal{P}^\mathcal{S}$ and $p_j^T \in \mathcal{P}^\mathcal{T}$ be two points of the respective sets. For each matching pair $(p_i^S, p_j^T)$, an infinite set of compatible affine transforms can be computed as follow:

$$\begin{bmatrix} p_j^T \\ \hline 1 \end{bmatrix} = \left[\begin{array}{c|c} \mathcal{R}(\theta_{ij}) & \begin{matrix} t_{x_{ij}} \\ t_{y_{ij}} \end{matrix} \\ \hline 0 & 1 \end{array}\right] \begin{bmatrix} p_i^S \\ \hline 1 \end{bmatrix} \qquad (13)$$

$$\begin{bmatrix} t_{x_{ij}} \\ t_{y_{ij}} \end{bmatrix} = p_j^T - \mathcal{R}(\theta_{ij}) p_i^S \qquad (14)$$

where $\mathcal{R}(\cdot)$ is a 2d rotation matrix. The Hough voting is performed varying $\theta_{ij}$ in the range $[\mathtt{min}_\theta, \mathtt{max}_\theta]$ and computing $t_{x_{ij}}$ and $t_{y_{ij}}$. Then, the matching pair $(p_i^S, p_j^T)$ is added in the Hough space element list with indexes $[t_{x_{ij}}, t_{y_{ij}}, \theta_{ij}]$. In particular, each subset of compatible affine transform given by the voting step can be seen as a helix in the three dimensional Hough space (Fig. 2). The optimal matching is given by the subset of matching pairs in the affine Hough space element with maximum cardinality.

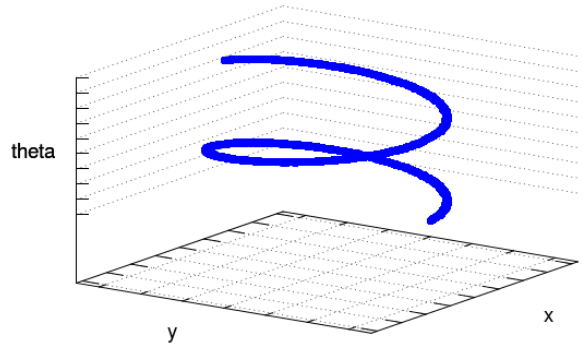


Fig. 2: An example of helix shape resulting with Hough voting algorithm in Affine Hough Transform.

## V. EXPERIMENTS

In this section we present our experimental setup and results based on loop-closure and map estimation. The experiments, are assessed in five public datasets: three indoor datasets (*fr079*, *intel*, *mit-csail*) and two outdoor (*fr-clinic*, *victoria-park*). The datasets, provided by [5], contain both original scans and corresponding corrected ground truth. Results are presented with precision-recall curves for loop-closure tests and with the resulting pose map for online map estimation.

### A. Experimental Setup

The loop-closure experiments are evaluated both comparing scans of the whole dataset (offline mode) and simulating an online map estimation:

- *Offline*. Each scan $\mathcal{S}_R$ of a dataset has been compared to the other candidate scans $\mathcal{S}_i$ with $i \neq R$.
- *Online*. Each scan $\mathcal{S}_R$ of a dataset has been compared to the other candidate scans $\mathcal{S}_i$ with $i < R$. To avoid trivial matching of consecutive scans we limit the loop-closure evaluation to those scans that have been registered in sufficiently far robot poses. Formally, let $[x_R, y_R, \theta_R]_R^\top$ and $[x_i, y_i, \theta_i]_i^\top$ be respectively the pose where reference scan $\mathcal{S}_R$ and candidate scan $\mathcal{S}_i$ have been registered; the loop-closure is evaluated only if at least one of the following conditions holds: $|x_R - x_i| > x_{th}$, $|y_R - y_i| > y_{th}$ or $|\theta_R - \theta_i| > \theta_{th}$.

The proposed loop-closure algorithms have been tested in each dataset and compared with two state-of-the-art algorithms, GFP and GSR. GSR is rather similar to the original GLARE and its performance has been already proven [9]. Hence, GLARE has not been evaluated in our experiments. First, we evaluate the original GFP and GSR algorithms using FLIRT keypoints and descriptors. Then, FALKO keypoints have been used as primitives in GSR signatures to evaluate how the higher stability of FALKO w.r.t. FLIRT keypoints influences place recognition performance. In all tests the improve FALKO detection with subbeam accuracy has been used. Finally, FALKO features with the proposed GLARE variant, GLAROT, has been evaluated with three different point-to-point matching methods: RANSAC, *Correspondence Graph* (CG) and *Affine Hough Transform* (AH). GFP and GSR variants use RANSAC algorithm as point-to-point association method.

For each algorithm, both offline and online loop-closure performance as the online global mapping has been evaluated. The loop-closure evaluation has been performed as follows. For each scan $\mathcal{S}$ of a dataset, the scan signatures have been computed and stored. Then, let $\mathcal{S}_R$ be the reference scan, a set $\mathcal{C}_S$ of 10 candidate scans (50 for GFP), whose signatures are closer to the signatures of the reference scan $\mathcal{S}_R$ according to the respective loop-closure method, are extracted. The set of closest signatures $\mathcal{C}_S$ is evaluated according to the corresponding distance function and thresholds of each loop-closure method. The keypoints of each scan in $\mathcal{C}_S$ are associated with $\mathcal{S}_R$ using the selected point-to-point association algorithm and are used to compute robot pose in least-squares sense. Finally, the scan selected for loop-closure $\bar{\mathcal{S}}_i$ is the scan that, after alignment, has the greatest number of keypoints with a neighbor point in $\mathcal{S}_R$ within the $0.10\ m$ range. The results of the loop-closure tests are shown with precision-recall curves. The robot is considered localized if the associated points are at least $N_{min}$. The precision-recall curves are computed w.r.t. the threshold $N_{min}$. A localization is considered correct when the position error of the aligned scan is less than $0.50\ m$ and the angular error less than $10°$.

Online map estimation is performed similarly to the loop-closure tests. First, a pose graph is constructed with the odometry poses provided by the datasets. Then, loop-closures have been evaluated as previously presented. In particular, if the selected scan $\bar{\mathcal{S}}_i$ has a number of associated points greater than $N_{th}$ then the loop is considered closed. The final pose graph is then optimized with the state-of-the-art SLAM back-end *g2o* [19].

### B. Loop-Closure Results

Loop-closure evaluation has been performed with default parameters for each algorithm. In particular, GFP, GSR and FALKO have been tested with corresponding recommended parameters [6], [7], [9]. RANSAC inlier probability for point-to-point association is set to 0.7. The tolerance $\epsilon$ of Correspondence Graph is set to $0.10m$. For Affine Hough Transform the searching range is set to $[-5m, 5m] \times [-5m, 5m] \times [-\frac{\pi}{2}, \frac{\pi}{2}]$; $\Delta_x$, $\Delta_y$ and $\Delta_\theta$ are set respectively to $0.1m$, $0.1m$ and $0.04rad$. Finally, for online loop-closure evaluation, $x_{th}$, $y_{th}$ and $\theta_{th}$ are set respectively to $0.20m$, $0.20m$ and $0.35rad$.

Figures 3 shows the offline and online results for loop-closure experiments with $N_{min}$ varying within the range $[0, 20]$. The top three rows are the results with indoor datasets whereas the last two rows are with outdoor ones. As can be seen, in offline mode (fig. 3.(a)) each algorithm performs slightly better than online. This is also possibly due to the avoidance of trivial associations between consecutive scans in online mode. GFP performs drastically different between offline and online. GFP computes the bag-of-words

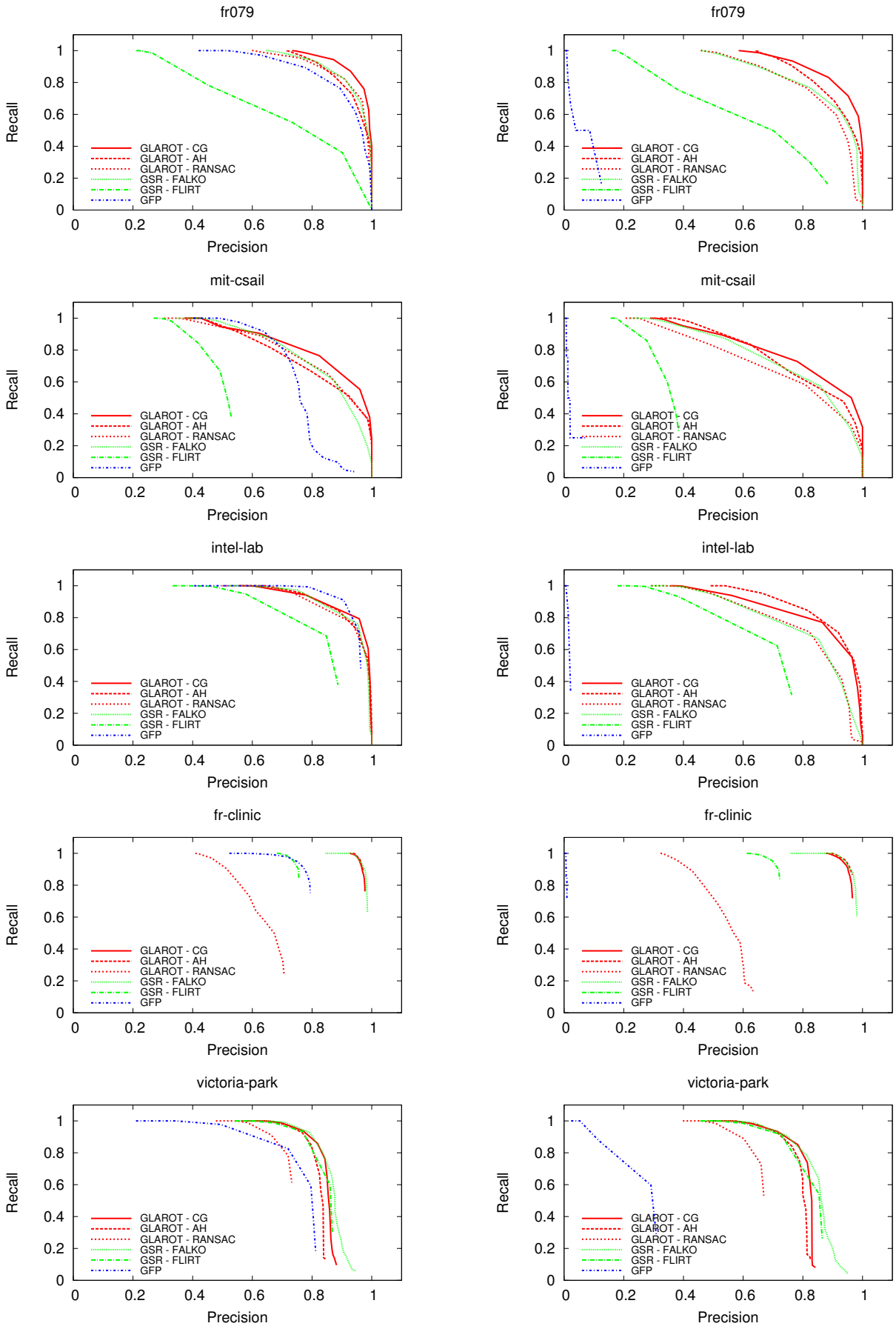


Fig. 3: Precision-Recall curves for offline (a) and online (b) loop-closure tests.

(BoW) using the whole dataset, and the availability of a limited number of phrases, inherent in online operation, causes this performance drop. Due to the higher stability and repeatability of FALKO keypoints w.r.t. FLIRT, GSR-FALKO outperforms GSR-FLIRT in all the datasets, except for *victoria-park* where the absence of corners in the environment leads to the same results for both algorithms. Finally, GLAROT (which is also based on FALKO keypoints) obtains almost always the best results in all the datasets. In particular, GLAROT-CG and GLAROT-AH slightly outperform GSR-FALKO and GLAROT-RANSAC, with GLAROT-CG obtaining higher precision and recall values, especially in indoor datasets.

### C. Online SLAM Results

This section illustrates the qualitative results of online map estimation. Except for *fr079*, figure 3.(b) shows the persistence of false positives in the loop closure results due to the limited number of revisited places. Even a single false loop detection drastically affects the final map reconstruction. Hence, the online SLAM results are shown only for *fr079* which provides reliable loop closure detection. Figure 4.(a) shows the correct ground truth [5], while the other images in figure 4 represent the map computed with the proposed loop-closure methods: GSR-FALKO, GLAROT-RANSAC, GLAROT-AH, and GLAROT-CG. Each algorithm has been evaluated choosing $N_{th}$ as the threshold generating the break even point in the corresponding precision-recall curve. Due to the persistent presence of false positives in the loop-closure results, maps generated by GFP and GSR-FLIRT are not shown. As can be seen in figures 4.(b)-(e), each method provides a valid optimization of the right side of the map, whereas in the left side the differences between algorithms are more pronounced. In particular, GLAROT-CG achieves the best global map estimation, also in the leftmost part of the map where loop closures are less frequent.

### D. Loop Closure Efficiency and FALKO Subbeam Accuracy

The efficiency of the algorithms has been empirically assessed by performing loop closure on on dataset *fr079*. The average execution times obtained with Intel i7-3630QM CPU @ 2.40GHz, 8 GB RAM are illustrated in Table I. Such values are affected by several parameters, including the total number of scans, the cardinality of the candidate set $\mathcal{C}_S$, the number of keypoints extracted from each scan. We report the average execution time per scan. The initialization of GFP takes significantly more time than the initialization of geometric signatures GLAROT and GSR. GFP is an intrinsically offline method that transfers most of the loop closure complexity to the computation of BoW histograms from the whole scan dataset. On the other hand, geometric signatures can be efficiently computed, since they only depend on the keypoints detected in a given scan. The complexity of closest signatures search depends on the number of scans in the set and is less efficient, but comparable with GFP association. Point-to-point association

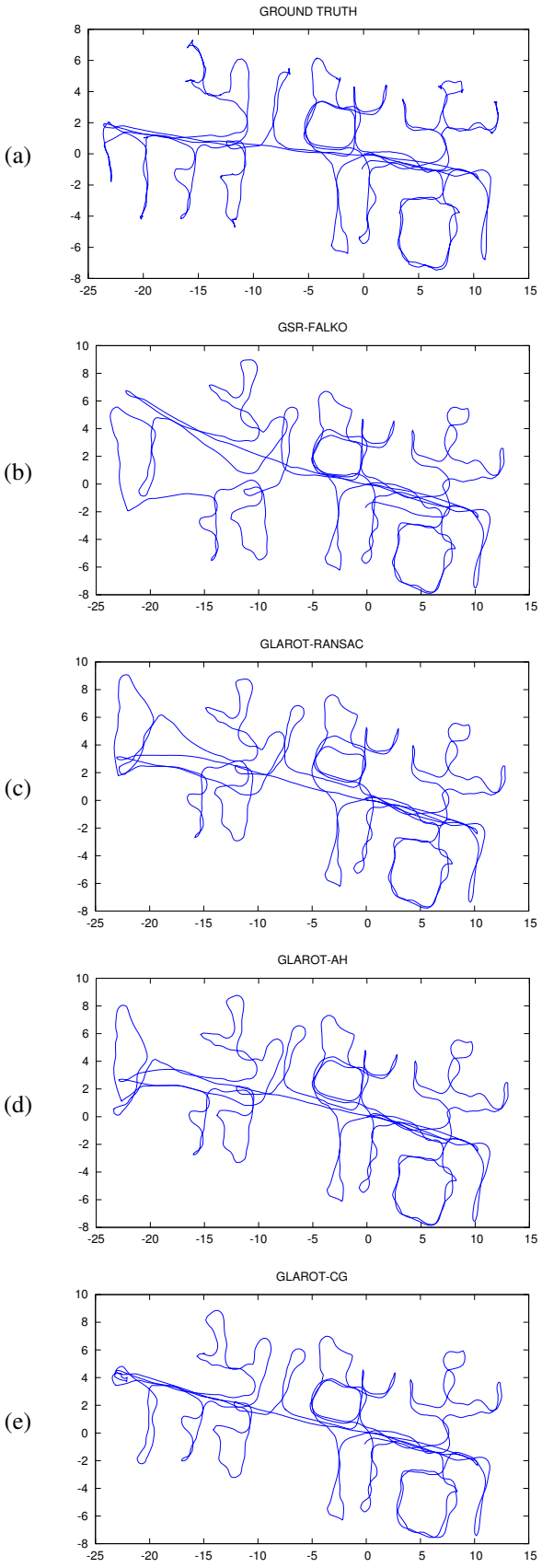


Fig. 4: Online SLAM pose map results for five algorithms: (a) ground truth provided by [5]; (b) GSR signatures using FALKO keypoints; (c) GLAROT with original RANSAC for point-to-point matching; (d) GLAROT with Affine Hough Transform; (d) GLAROT with Correspondence Graph.

| operation | | # candidate | avg time [ms] |
|---|---|---|---|
| GFP | creation | - | 2.702 |
| | association | 50 | 2.376 |
| GSR | creation | - | 0.123 |
| | association | 10 | 36.204 |
| GLAROT | creation | - | 0.123 |
| | association | 10 | 12.154 |
| CG | | 10 | 16.314 |
| AH | | 10 | 356.927 |
| RANSAC | | 10 | 49.430 |

TABLE I: Average times per scan required for creation, signature and point-to-point association using different methods in offline experiments with dataset fr079.

| dataset | position [cm] | | |
|---|---|---|---|
| | avg | std dev | max |
| fr079 | 2.88 | 3.39 | 19.96 |
| mit-csail | 3.42 | 3.91 | 38.18 |
| intel-lab | 2.88 | 2.91 | 19.99 |
| fr-clinic | 1.41 | 3.69 | 20.01 |
| victoria-park | 1.29 | 3.60 | 20.00 |

TABLE II: Average, standard deviation and maximum distance between FALKO keypoints computed using subbeam accuracy and keypoints computed based on beam resolution for all datasets.

is the most computationally demanding step of loop closure. CG has proven more efficient than AH and RANSAC.

All the presented loop closure methods associate keypoint pairs assuming a given tolerance between points (e.g. RANSAC acceptance threshold or correspondence graph compatibility). Thus, the proposed subbeam technique illustrated in section III-B does not affect directly loop closure capability, but can improve scan registration and the accuracy of landmark position. We have compared the FALKO keypoints position obtained using the subbeam technique and using beam resolution. The results for all the datasets are shown in Table II. The average distance is between $1.3$ and $3.5$ $cm$ with a standard deviation below $4$ $cm$.

## VI. CONCLUSION

In this paper, we have illustrated novel loop closure methods based on FALKO keypoints and compared their performance in both offline and online localization and mapping problems. An improved version of FALKO detector, which uses subbeam evaluation, is proposed and used as a reliable input to place recognition algorithms. The FALKO keypoints detected from each laser scan become part of a corresponding local map. To find loops, i.e. regions already visited by the robot, the current local map is matched with the other local maps in two steps. The candidate loops are found by comparing signatures and, then, point-to-point association is applied to match individual keypoints and to compute the accurate rigid transformation between local maps. The novel signature GLAROT has also been proposed and compared with state-of-the-art signature algorithms. Moreover, several point-to-point data association techniques have been evaluated. Experimental results obtained from publicly available datasets have assessed performance of loop closure methods applied to both offline and online localization and mapping problems. Online place recognition imposes stronger constraints over results and has not been addressed in previous works based on laser keypoints. Results show that the stability of FALKO keypoints has proven crucial for loop closure. FALKO detector combined with GLAROT signature and point-to-point association outperforms the other approaches.

## VII. ACKNOWLEDGEMENTS

We want to thank Prof. Stefano Caselli for his support in the discussion and review of this work.

## REFERENCES

[1] J.-S. Gutmann and K. Konolige, "Incremental Mapping of Large Cyclic Environments," in *Proc. of the IEEE Int. Symposium on Computational Intelligence in Robotics and Automation (CIRA)*, 1999, pp. 318–325.

[2] D. Lodi Rizzini and S. Caselli, "Metric-topological maps from laser scans adjusted with incremental tree network optimizer," *Robotics & Autonomous Systems*, vol. 57, no. 10, pp. 1036 – 1041, 2009.

[3] D. Hähnel, S. Thrun, B. Wegbreit, and W. Burgard, "Towards lazy data association in SLAM," in *Proc. of the International Symposium on Robotics Research (ISRR)*, 2003.

[4] G. Grisetti, C. Stachniss, and W. Burgard, "Improved Techniques for Grid Mapping with Rao-Blackwellized Particle Filters," *IEEE Trans. on Robotics*, vol. 23, no. 1, pp. 34–46, 2007.

[5] G. D. Tipaldi and K. O. Arras, "Flirt-interest regions for 2d range data," in *Proc. of the IEEE Int. Conf. on Robotics & Automation (ICRA)*, 2010, pp. 3616–3622.

[6] F. Kallasi, D. Lodi Rizzini, and S. Caselli, "Fast keypoint features from laser scanner for robot localization and mapping," *RAL*, vol. 1, no. 1, pp. 176–183, jan 2016, dOI 10.1109/LRA.2016.2517210.

[7] G. D. Tipaldi, L. Spinello, and K. O. Arras, "Geometrical flirt phrases for large scale place recognition in 2d range data," in *Proc. of the IEEE Int. Conf. on Robotics & Automation (ICRA)*, 2013, pp. 2693–2698.

[8] M. Himstedt, J. Frost, S. Hellbach, H.-J. Boehme, and E. Maehle, "Large scale place recognition in 2D lidar scans using geometrical landmark relations," in *Proc. of the IEEE/RSJ Int. Conf. on Intelligent Robots and Systems (IROS)*, 2014, pp. 5030–5035.

[9] M. Himstedt and E. Maehle, "Geometry matters: Place recognition in 2D range scans using Geometrical Surface Relations," in *Proc. of the European Conference on Mobile Robots (ECMR)*, 2015, pp. 1–6.

[10] M. Bosse and R. Zlot, "Map Matching and Data Association for Large-Scale Two-dimensional Laser Scan-based SLAM," *Int. Journal of Robotics Research*, vol. 27, no. 6, pp. 667–691, Jun 2008.

[11] ——, "Keypoint design and evaluation for place recognition in 2D LIDAR maps," *Robotics & Autonomous Systems*, vol. 57, no. 12, pp. 1211–1224, 2009.

[12] Y. Li and E. Olson, "Extracting general-purpose features from LIDAR data," in *Proc. of the IEEE Int. Conf. on Robotics & Automation (ICRA)*, 2010.

[13] ——, "Structure tensors for general purpose lidar feature extraction," in *Proc. of the IEEE Int. Conf. on Robotics & Automation (ICRA)*, 2011, pp. 1869–1874.

[14] J. Neira and J. Tardós, "Data Association in Stochastic Mapping Using the Joint Compatibility Test," *IEEE Trans. on Robotics*, vol. 17, no. 6, pp. 890–897, 2001.

[15] T. Bailey, E. Nebot, J. Rosenblatt, and H. Durrant-Whyte, "Data association for mobile robot navigation: a graph theoretic approach," in *Proc. of the IEEE Int. Conf. on Robotics & Automation (ICRA)*, 2000, pp. 2512–2517.

[16] L. Paz, P. Pinies, J. Neira, and J. Tardos, "Global localization in slam in bilinear time," in *Proc. of the IEEE/RSJ Int. Conf. on Intelligent Robots and Systems (IROS)*, Aug 2005, pp. 2820–2826.

[17] R. Duda and P. Hart, "Use of the hough transformation to detect lines and curves in pictures," *Commun. ACM*, vol. 15, no. 1, pp. 11–15, Jan 1972.

[18] D. H. Ballard, "Generalizing the hough transform to detect arbitrary shapes," *Pattern Recognition*, vol. 13, no. 2, pp. 111 – 122, 1981.

[19] R. Kuemmerle, G. Grisetti, H. Strasdat, K. Konolige, and W. Burgard, "g2o: A General Framework for Graph Optimization," in *Proc. of the IEEE Int. Conf. on Robotics & Automation (ICRA)*, 2011.